Original Paper *Forma*, **16**, 17–46, 2001

Mathematical Index and Model in Stabirometry

Hiroki TAKADA[1], Yoshiyuki KITAOKA[2] and Yuuki SHIMIZU[3]

[1]*Graduate School of Mathematics, Nagoya University, Chikusa-ku, Nagoya 464-8602, Japan*
[2]*Department of Mathematics, Meijo University, Tempaku-ku, Nagoya 468-8502, Japan*
[3]*Institute for Hydrospheric-Atmospheric Sciences, Nagoya University, Chikusa-ku, Nagoya 464-8601, Japan*

(Received April 20, 2000; Accepted March 21, 2001)

Keywords: Sway of the Center-of-Gravity of the Body, Stabirometry, Fokker-Planck Equation (FPE), Stochastic Dynamical Equation (SDE), Form of a Potential Function

Abstract. We measured the sway of the center-of-gravity of the body with a stabirometer for five men aged of 19 to 25 years. There are standardized parameters on stabirometry (observation with the stabirometer) by SUZUKI *et al*. (1996). We have analyzed the measured data by paying attention to *force* acting on it. We could admit *polarity* and *rhythm* on the force and the kind of effect of visual information. We also constructed a mathematical model of the sway of the center-of-gravity of the body on some conditions. We obtained a stochastic dynamical equation system as a mathematical model corresponding to the sway of the center-of-gravity of the body. We compared the statokinesigram obtained from the numerical simulation of this SDE with that obtained from the measured data.

1. Introduction

The man's standing posture is maintained by an involuntary physiological adjustment mechanism. The evaluation of this function is indispensable for diagnosing patients with equilibrium disturbance like giddiness and Parkinson's disease. An inspection method with a stabirometer is used as qualitative and quantitative evaluation.

The stabirometer is an observation system that measures a projection of a subject onto a detection-stand, a ground-based two-dimensional plane $\boldsymbol{E}^2$, for each time step. The sway of the center-of-gravity of the body measured by this system is recorded as the sway of the center-of-gravity of the body on the Euclidean plane $\boldsymbol{E}^2$. In this paper, the sway of the center-of-gravity of the body projected on $\boldsymbol{E}^2$ is referred as the sway of the center-of-gravity.

Kinematical analysis of the sway of the center-of-gravity is important not only on medicine but also elucidation of control of a standing upright as a two-legs robot. The application of this research is also valuable to these studies.

Parameters on analysis of stabirometry, like total locus length and area of sway, are standardized by SUZUKI *et al*. (1996) and they are widely used for clinical studies (MORI *et al*., 1998). Other mathematical parameters are used for the analysis on the sway of the center-of-gravity. For example, TAKEUCHI *et al*. (1997) have composed attractors of the sway of the center-of-gravity and resulted that they are neither the systematic nor complete white noise by calculating each Lyapunov's number and fractal dimension. We have shown that this sway is unable to be described as any harmonic oscillator systems with a statistical method (TAKADA and SHIKATA, 1998) and pointed out that it is possible that skeletal structure of feet is related to the sway of the center-of-gravity with a geometrical index, a *rotation angle* that is defined at the next section (SHIKATA *et al*., 1997). Some previous researchers tried to describe the sway of the center-of-gravity with a stochastic model. We will mention that the previous model is premature as a description on the control system in a certain dynamical system in Subsection 6.2. In spite of these studies, the mathematical model on the sway of the center-of-gravity has not been established yet. The purpose of this research is to analyze the sway of the center-of-gravity by paying attention to *force* acting on the center-of-gravity and constructing its mathematical model. We are going to compare the previous model with our model and show validity of our model in that section.

2. Measurement of the Sway of the Center-of-Gravity

We analyzed the sway of the center-of-gravity by paying attention to *force* in this research. First, we discuss a method for calculation of force acting on the center-of-gravity from measured data with stabirometer. Force can be considered as acceleration under the second law of motion; therefore we consider a difference of two displacement vectors as *force* acting on the center-of-gravity. In other words, *force* acting on the center-of-gravity on a discrete system can be defined:

Definition 1 Positions of the center-of-gravity at time steps $t - 1$, t and $t + 1$ are defined as P_{t-1}, P_t and P_{t+1} ($\in \boldsymbol{E}^2$). The difference of two displacement vectors: $\overrightarrow{P_{t-1}P_t}$ and $\overrightarrow{P_tP_{t+1}}$ is defined as *force* acting on the center-of-gravity at time t (Fig. 1):

$$\boldsymbol{f}_t = \overrightarrow{P_tP_{t+1}} - \overrightarrow{P_{t-1}P_t}.$$

The angle between vectors: $\overrightarrow{P_{t-1}P_t}$ and $\overrightarrow{P_tP_{t+1}}$ is assumed to be a *rotation angle* θ_t (at time t) which means the curvature if all norms of vectors $\overrightarrow{P_{t-1}P_t}$ are 1, where clockwise as positive.

Definition 2 K is a set of sampling time when we have observed the positions of the center-of-gravity. However, a set K does not contain both time extent when the subject stands with eyes shut and with eyes opened at the same time. A *projection of force* $\boldsymbol{f}_t$ *onto the direction of angle* j on the discrete system is defined as (Fig. 2):

$$f_t(j) = f_t^x \cos j + f_t^y \sin j,$$

where $j = 0°–175°$ with the interval of angle 5° and f_t^x, f_t^y are components of the *force* on $\boldsymbol{E}^2$ (i.e. $\boldsymbol{f}_t = {}^t(f_t^x f_t^y) \in \boldsymbol{E}^2$). The *Sum total of force onto the direction of angle* j is defined as:

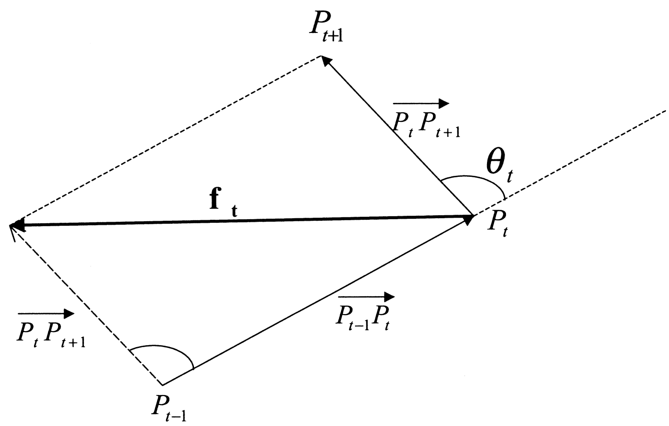

Fig. 1. The difference between two displacement vectors is defined as *force* acting on the center-of-gravity. We call the angle θ_t a *rotation angle* that is related to the curvature where clockwise as positive.

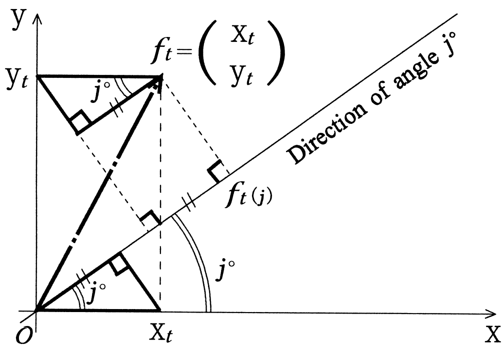

Fig. 2. A projection of *force* $\boldsymbol{f}_t$ onto the direction of angle $j°$ on a discrete system is shown in this figure where clockwise as negative.

$$f(j;K) = \sum_{t \in K} |f_t(j)|.$$

Next, we mention how to measure the sway of the center-of-gravity. We used a gait analysis system (Force Plate) manufactured by the AMTI Co. Ltd. as a stabirometer. The sway of the center-of-gravity is recorded as coordinates $(x_t y_t)$ on $\boldsymbol{E}^2$ (*xy* plane) at each time step. A subject stands on the detection-stand and the coordinates of the center-of-gravity are measured with a number of strain gauges in it. Their outputs are amplified by a biomechanics amplifier and simultaneously recorded with an A-D converter through a low-pass filter (10 Hz). In this way, the displacement of the center-of-gravity projected on *xy*

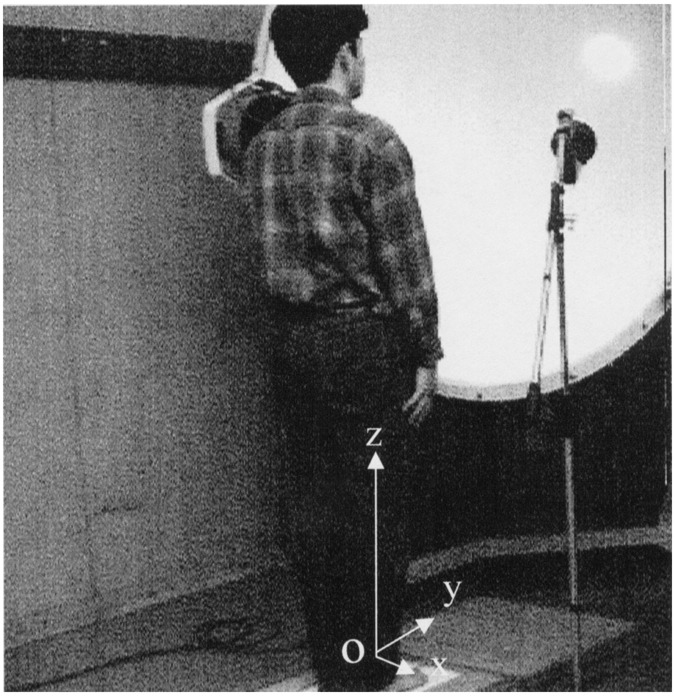

Fig. 3. We show the Cartesian coordinates system in the observation system in this figure. The detection stand was horizontally fixed on the flat floor. We measured in the quiet room. Under such conditions, the center-of-gravity profiles by a standing person with Romberg's posture were measured for 5 men. The fixation point was set at height of subject's eyes and two meters ahead.

plane is recorded for each time step. The reading error of the center-of-gravity is 0.2 centimeters on this system.

Therefore, the sway of the center-of-gravity is recorded as the data on *xy* plane. However, components of the displacement on three-dimensional Euclidean space $\boldsymbol{E}^3 \ni (x, y, z)$ are also needed for analysis. We assumed subject's glance to be a positive direction of *y* axis. Based on the right-handed system, other axes (*x*, *z*) were defined as shown in Fig. 3. The vertical component of the center-of-gravity of the subject on the detection-stand $\vec{r_g}$ is defined as:

$$\vec{r_g} = \left(-\frac{N_y}{F_z}, \ \frac{N_x}{F_z} \right),$$

where $\boldsymbol{F} = (F_x, F_y, F_z)$ is a vector of the sum total of external force acting on a detection-stand and $\boldsymbol{N} = (N_x, N_y, N_z)$ is a vector of the moment of the external force.

Subjects were healthy five men aged of 19 to 25 years. A subject stood in standing posture with his foot shut, what is called Romberg's posture, on a detection-stand and his sway of the center-of-gravity was recorded individually. A fixation point for the state with eyes opened was set with laser pointer at height of subject's eyes and two meters ahead. Programs of measurement are as follows.

Measurement 1 The subject stands for 20 [s] with eyes opened and subsequently for 20 [s] with eyes shut for three turns alternately. A point of the center-of-gravity is recorded for each 0.025 [s] and the each data set consists of 800 points. We assume the number of time extent to be M for analysis. Subject stands with eyes opened for time extents of odd numbers and eyes shut for evens.

Measurement 2 The subject stands for 60 [s] with eyes opened, subsequently for 60 [s] with eyes shut. We recorded the sway of the center-of-gravity on this time. A point of the center-of-gravity is recorded for each 0.05 [s]. This measurement is established by SUZUKI *et al*. (1996).

We do not record the data for 5 [s] after changing from the state with eyes shut to open not to analyze transient response phenomenon with reflex of the visual stimulation in Measurement 1.

3. Analysis of the Sway of the Center-of-Gravity

Some characteristics of the *force* acting on the center-of-gravity are clarified with by calculating the *sum total of force* on the time series of the sway of the center-of-gravity measured with Measurements 1 and 2 mentioned above.

3.1. Polarity of force acting on the center-of-gravity

At first, we analyzed the data obtained with Measurement 1. We calculated $f(j, K^M)$ for all j and M ($M = 1, ..., 6$) and plotted them in polar graphs (to display the data in polar coordinates) of each subject and M (Fig. 4(a)). Each graph was not isotropic but convex distortion appeared in a certain direction remarkably. *Polarity* appeared on the *force* acting on the center-of-gravity. In the rest of the paper, the direction of the largest $f(j, K^M)$ is referred as the *direction of polarity*.

We have also calculated the ratio $f(j, K^{M+1})/f(j, K^M)$, where M is an odd number ($M = 1, 3, 5$) for eyes opened. We have found the tendency that the ratio falls less than 1 on any directions as increment of M (Fig. 5).

We analyzed the data obtained with Measurement 2. In order to detect the time dependency of $f(j, K^M)$, a span of the calculation was set to 10 [s]. Here, we introduce time-localized $f(j, K_t^Q)$ where the suffix t is an onset time of the interval and Q is defined as follows.

$$Q = \begin{cases} 1 & (\text{with eyes opend}) \\ 0 & (\text{with eyes shut}). \end{cases}$$

(a)

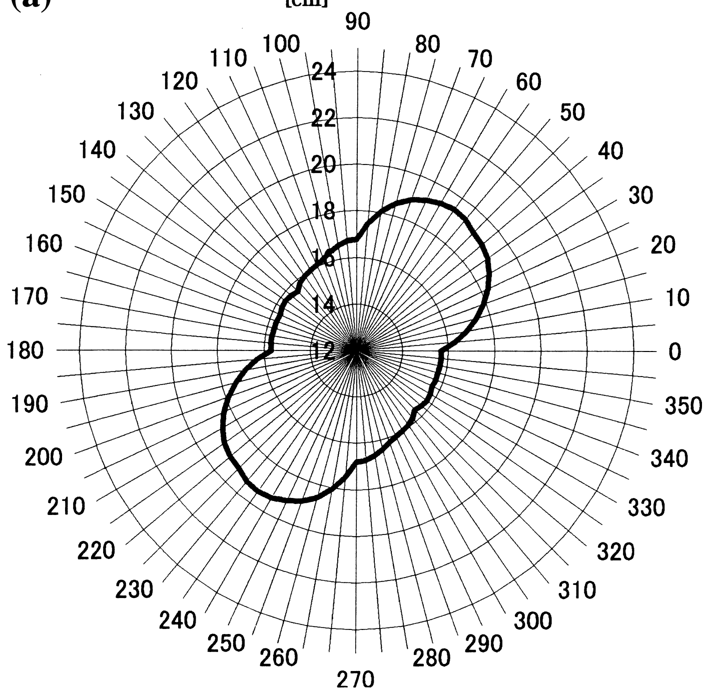

Fig. 4. We analyzed the time series data with Measurement 1 on Fig. 4(a) and with Measurement 2 on the other figures. We calculated each *sum total of force onto the direction of angle j°*. We show each *sum total of force* on these polar graphs. *Polarity* was admitted on any graphs. On each graph, the conditions of each experiment and subjects' initials are as follows: (a) Subject was Y.S. (19 years old) at the first experiment ($M = 1$). (b) Subject was H.H. (20 years old) with his eyes open. We could also admit rotation on the direction of polarity on this figure. (c) Subject was H.H. (20 years old) with his eyes shut.

We calculated $f(j, K_t^Q)$ for $j = 0°–175°$ at intervals of 5°, $t = 0–50$ at intervals of 10 [s] and $Q = 1,0$, and plotted them on a polar graph for each subject, t and Q (Figs. 4(b) and (c)). The *Polarity* was admitted on any graph. Also, rotation on the *direction of polarity* was found for eyes opened (Fig. 4(b)). Therefore, we can suggest that peculiar strategy in standing posture depends on visual information.

3.2. Rhythm on force acting on the center-of-gravity

In order to declare time variation of $f(j, K_t^Q)$, we calculated moving averages on the *sum total of force onto the direction of* 0° and 90° for 60 [s]. A span of the moving average was set to 10 [s]. In other words, we calculated $f(j, K_t^Q)$ for $j = 0°, 90°$, $t = 0.05–49.95$, where the interval of the onset time t was 0.05 [s] and $Q = 1,0$. We sequentially arranged $f(j, K_t^Q)$ of each j and Q for smaller t, and obtained the time series data $\{f(j, K_t^Q)\}_{t=0.05}^{49.95}$. Obvious periodicity (*rhythm*) of this time series $\{f(j, K_t^Q)\}_{t=0.05}^{49.95}$ for each j and Q was admitted

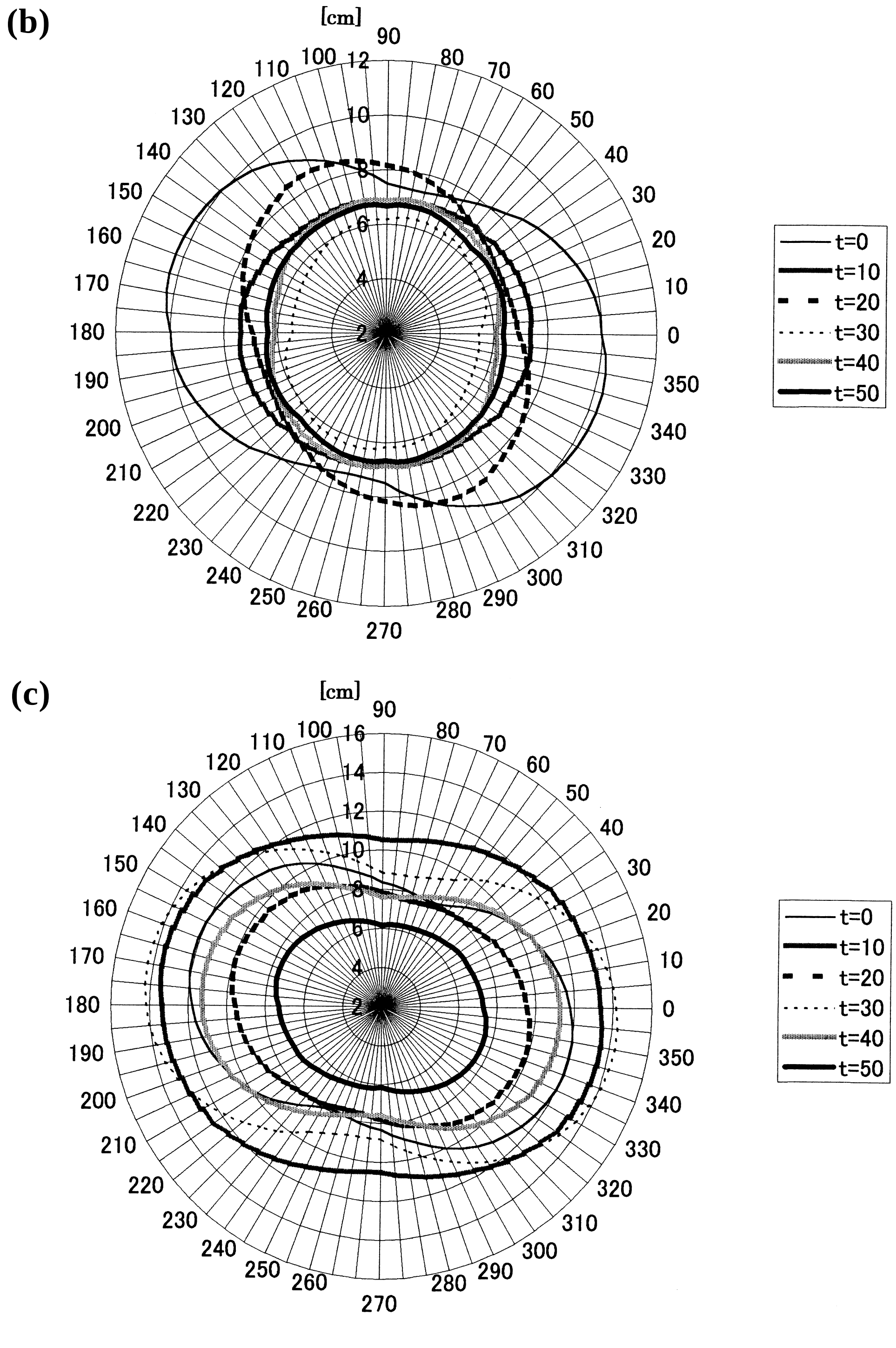

Fig. 4. (continued).

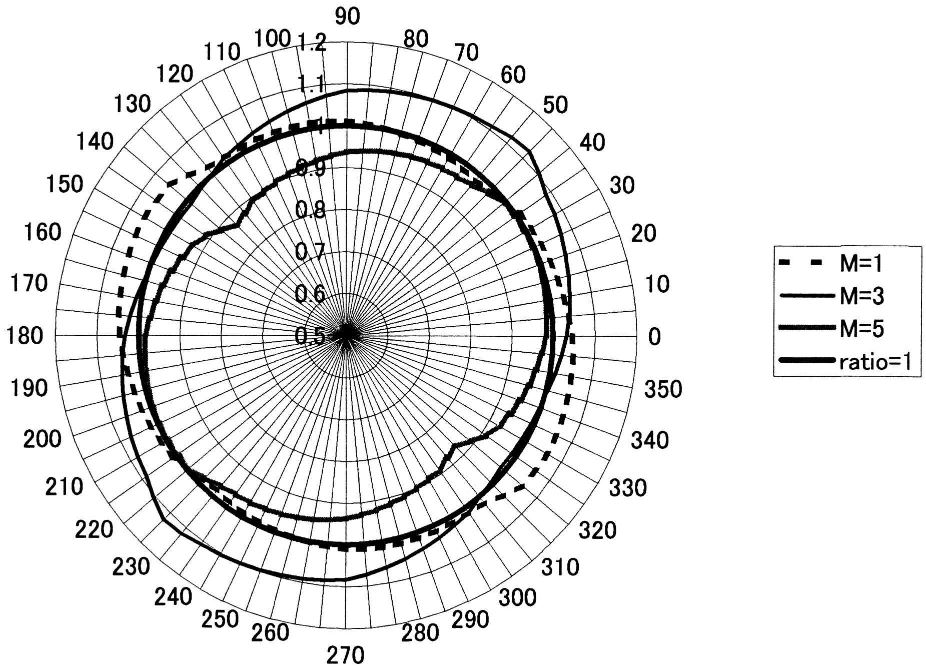

Fig. 5. We analyzed the time series data with Measurement 1. Subject was T.N. (25 years old). The ratios $f(j, K^{M+1})/f(j, K^{M})$ (M = 1, 3, 5) were plotted in this figure. Though the ratios in any directions were more than 1 at the first experiment (M = 1), any ratios were less than 1 at the third experiment (M = 5).

(Fig. 6). Here, in order to declare the *rhythm* of the *force* acting on the center-of-gravity, we have employed the discrete Fourier transform (DFT) of $\{f(j, K_t^Q)\}$. However, the interval of this moving average has been set as 8.75 [s] for the convenience of FFT that is a fast radix-2 fast-Fourier transform algorithm just in case the length of data is a power of two. Power spectrums of the time series $\{f(0°, K_t^Q)\}_{0.05}^{51.25}$ for each are shown in Fig. 7. We compared these power spectrums corresponding to each time series $\{f(0°, K_t^1)\}_{0.05}^{51.25}$, $\{f(0°, K_t^0)\}_{0.05}^{51.25}$ in this figure.

Here, we could admit the *polarity* and the *rhythm* on the *force* acting on the center-of-gravity with the established measurement (SUZUKI *et al.*, 1996) by calculating our proposed indices mentioned above.

4. Construction of the Mathematical Model

In this section, we mention a construction of the mathematical model for postural center-of-pressure profiles by each upright, bipedal, standing person. The model is based on the stochastic theory. Definition and assumptions on the model are as follows.

Fig. 6. We analyzed the time series data with Measurement 2 and calculated the *sum total of force onto the direction of angle* 0°. Subject was S.I. (22 years old). We show typical time series of moving averages on the *sum total of force* for $Q = 1$ (with his eyes open) in this figure. There, *rhythm* on this time series was admitted.

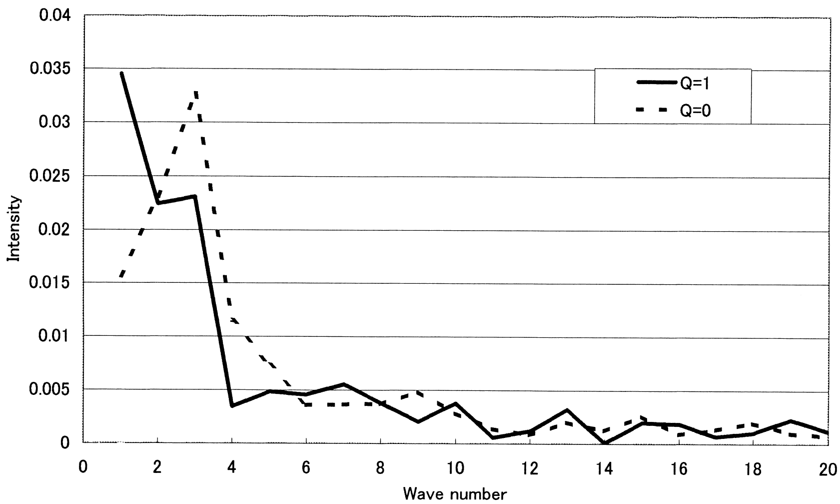

Fig. 7. We show the power spectrum of time series of moving averages on the *sum total of force* (see Fig. 6) for each Q.

Definition 3 We consider a continuous stochastic process on state space Ω. We assume a conditional probability to be $P(x|y, t)$ in such case as the random process $X(t)$ satisfies conditions of $X(0) = y$ $(\in \Omega)$ and $X(t) = x$ $(\in \Omega)$.

Assumption 1 The described stochastic process is one of Markov processes (Markovian).

Assumption 2 $X(t)$ is not an anomalous process that extends rapidly far in short time.

4.1. Fokker-Plank equation

If the above is assumed, the stochastic process $X(t)$ can be described by the following stochastic differential equation, what is called a Fokker-Plank equation (FPE) after all.

$$\frac{\partial P(x|y,t)}{\partial t} = -\frac{\partial}{\partial x}\left[a(x)P(x|y,t)\right] + \frac{1}{2}\frac{\partial^2}{\partial x^2}\left[b(x)P(x|y,t)\right]. \tag{1}$$

We can consider that the stochastic process $X(t)$ on Eq. (1) is not an anomalous-diffusion process (Appendix A). We will treat such processes as follows. Equation (1) goes over into Eq. (2) with the permutation of variables (Appendix B). There, we transform the random variable x into z:

$$\frac{\partial g(z|z_0,t)}{\partial t} = -\frac{\partial}{\partial z}\left[\hat{a}(z)g(z|z_0,t)\right] + \frac{1}{2}\frac{\partial^2}{\partial z^2}g(z|z_0,t) \equiv -\frac{\partial}{\partial z}J(z|z_0,t), \tag{2}$$

where $g(z|z_0, t)$ is a probability density function (PDF) transformed from $P(x|y, t)$ and z_0 is the initial condition. Since this equation is the equation of continuity on the PDF, $J(z|x, t)$ means flow of the probability and the stationary value $J(z|x, \infty) \equiv J(\infty)$ is a constant. A strict stationary solution of Eq. (2) can be obtained.

Theorem 1 (HARKEN, 1975) The stationary solution of Eq. (2) is as follows:

$$g(z) = \left\{C - 2J(\infty)\int_\Omega \exp\left[-2\int_\Omega \hat{a}(\xi)d\xi\right]dz\right\}\exp\left[2\int_\Omega \hat{a}(\xi)d\xi\right],$$

where C is a normalization factor defined with the formula:

$$\int_{-\infty}^{\infty} g(\xi)d\xi = 1.$$

Under a natural boundary condition such as $J(\pm\infty) = 0$, the stationary solution of Eq. (2) is as follows:

$$g(z) = C\exp\left[2\int^z \hat{a}(\xi)d\xi\right]. \tag{3}$$

4.2. Stochastic dynamical equation

Equation (2) can be led by calculating moments of transition probability $M_n(z)$ on the process that a stochastic dynamical equation (SDE) describes (GOEL and RICHTER-DYN, 1978). We define the moment $M_n(z)$ for degree n (a natural number) in Appendix A and the SDE here. In general, the SDE can be also written as a first-order differential equation that depends on a random variable z and fluctuating force $F(t)$ in the inhomogeneous term:

$$\frac{dz(t)}{dt} = G(z, F(t)), \tag{4}$$

where $F(t)$ is standardized fluctuating force generated with a Gauss type stochastic process. Strict definition of $F(t)$ is mentioned by the amounts of the following time averages:

$$\langle F(t) \rangle = 0,$$

$$\langle F(t)F(t+\tau) \rangle = \delta(\tau),$$

and more than third order correlations of $F(t)$ are 0 (GOEL and RICHTER-DYN, 1978). The angled brackets $\langle \bullet \rangle$ denote on the average over time. We can easily formulate a difference equation from the first-order differential equation; therefore Eq. (4) is an advantageous expression for the numerical computation. The computations give numerical solutions of the SDE, which are not probability density functions but movement of the variable. We can compare the solutions with the time series data and verify our theory.

The problem finding the SDE corresponding to a given FPE does not have a solution uniquely. However, the solution is unique if we limit the SDE as a type of following additive formula, which is described as a sum of a function on the variable z and the fluctuating force.

$$\frac{dz(t)}{dt} = \hat{a}(z) + F(t). \tag{5}$$

In previous researches, the function $\hat{a}(z)$ is linear, and then Eq. (5) can be rewritten as a mathematical model that describes one of Ornstein-Uhlembeck (OU) processes:

$$\frac{dz(t)}{dt} = -\gamma z + F(t). \tag{6}$$

However, in this research $\hat{a}(z)$, is assumed non-linear.

We also have the following advantages by separating $\hat{a}(z)$ and $F(t)$ in the inhomogeneous term on the SDE (4):

- We obtain the additive formula (5) of the SDE as theoretical extension on a gradient system (TAKADA, 2001).
- We obtain the advantageous expression (5) to the following consideration on mathematical meaning of the coefficient function $\hat{a}(z)$ on Eq. (2).

We discuss the mathematical meaning of the coefficient function on Eq. (2) here. With the operation of the SDE corresponding to the FPE (2), the second term of the right-hand side on Eq. (5) goes to 0 if we take time averages of both sides of this equation. With Stratonovich's rule (STRATONOVICH, 1963), Eq. (5) can be rewritten into an ordinary differential equation (ODE) on $\langle z \rangle$, the time average of the random variable z. $\hat{a}(z) = 0$ is equilibrium space of the ODE. On Eq. (5), $\hat{a}(z) = 0$ means the equilibrium space in the meaning of the time average. Hence, the space integral of the coefficient function $\hat{a}(z)$:

$$V(z) = -\int^{z} \hat{a}(\xi) d\xi \tag{7}$$

is a potential function in the meaning of the time average on Eq. (5). Equation (3) can be rewritten as a relation between a stationary probability density function (SPDF) and the potential function:

$$g(z) = C \exp[-2V(z)]. \tag{8}$$

Therefore, the following proposition is obtained by differentiating both sides of Eq. (8) (TAKADA, 2001).

Proposition 1 The number of stationary points and their positions z on the potential function $V(z)$ and on the SPDF $g(z)$ are corresponding.

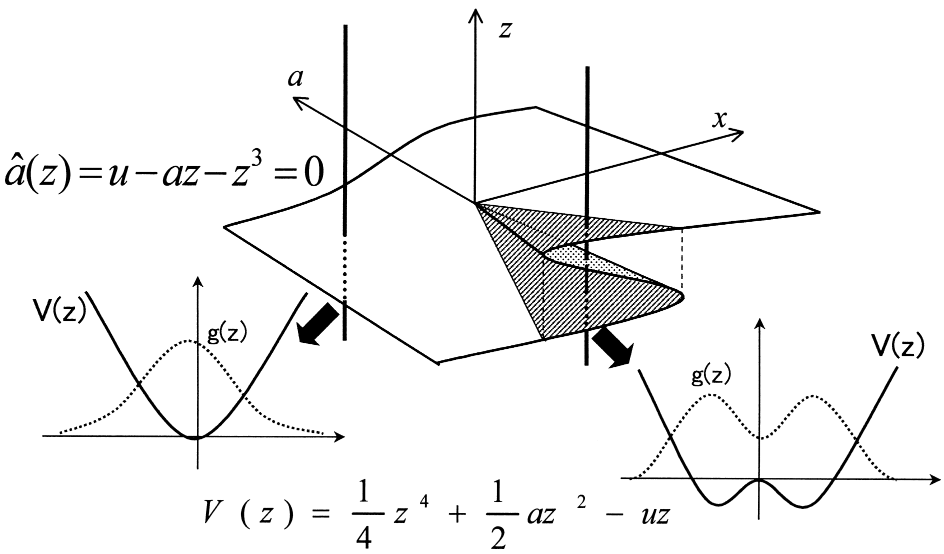

Fig. 8. The form of the potential function corresponds to the form of the probability density function. The zero points of derivative of the potential function construct the equilibrium space. On the example shown in this figure, the equilibrium space is Riemann-Hugoniot's manifold.

Here, we show an example on the correspondence between $V(z)$ and $g(z)$ in Fig. 8. Equilibrium space $\hat{a}(z) = u - az - z^3 = 0$ is, what we call, Riemann-Hugoniot's manifold (POSTON and STEWART, 1978). The potential function corresponding to this manifold is derived:

$$V(z) = \frac{1}{4}z^4 + \frac{1}{2}az^2 - uz,$$

by Eq. (7). This potential function $V(z)$ has two minimal points as $a < 0$ and $u \in ((-2|\alpha|\sqrt{|\alpha|/3}/3), (2|\alpha|\sqrt{|\alpha|/3})/3)$. Then, the SPDF $g(z)$ has two maximal points in this case. Otherwise, $V(z)$ has a minimal point and $g(z)$ has a maximal point.

Many of data that expected to be described with a SDE seem to be in a certain dynamical equilibrium state. The SPDF $g(z)$ can be obtained with a normalized histogram of time series practically. With Proposition 1, the form of the graph of $\log g(z)$ corresponds to the form of the graph of the potential function $V(z)$ in the meaning of time average on Eq. (5) that describes the process. We can consider Eq. (5) that is constructed with the time series data as the SDE corresponding to it.

5. Our Mathematical Model of the Sway of the Center-of-Gravity

The above-mentioned theory can be applied to a construction of the mathematical model corresponding to the sway of the center-of-gravity.

5.1. Verification of assumptions with measured data

First, we examined independency of coordinates on the time series of the center-of-gravity $\{(x_t, y_t)\}_{t\in K}$, that are needed for two-dimensional descriptions on this mathematical model. The independency can be examined with cross-correlation coefficients $\rho_{xy}(k)$ between series $\{x_t\}_{t\in K}$ and $\{y_t\}_{t\in K}$:

$$\rho_{xy}(k) = \frac{\sum_{i=k}^{N}\left\{x(i) - \langle x\rangle_k\right\}\left\{y(i-k) - \langle y\rangle_k\right\}}{\sqrt{\sum_{i=k}^{N}\left\{x(i) - \langle x\rangle_k\right\}^2}\sqrt{\sum_{i=k}^{N-k}\left\{y(i) - \langle y\rangle_k\right\}^2}},$$

where k is lag-time, N is the number of data points and $\langle x\rangle_k$, $\langle y\rangle_k$ are averages of the variable x, y in each domain given by the following expression:

$$\langle x\rangle_k = \frac{1}{N-k+1}\sum_{j=k}^{N}x(j), \quad \langle y\rangle_k = \frac{1}{N-k+1}\sum_{j=0}^{N-k}y(j).$$

According to nerve physiology, it takes 80 [ms] until the signal input from sensory nerves

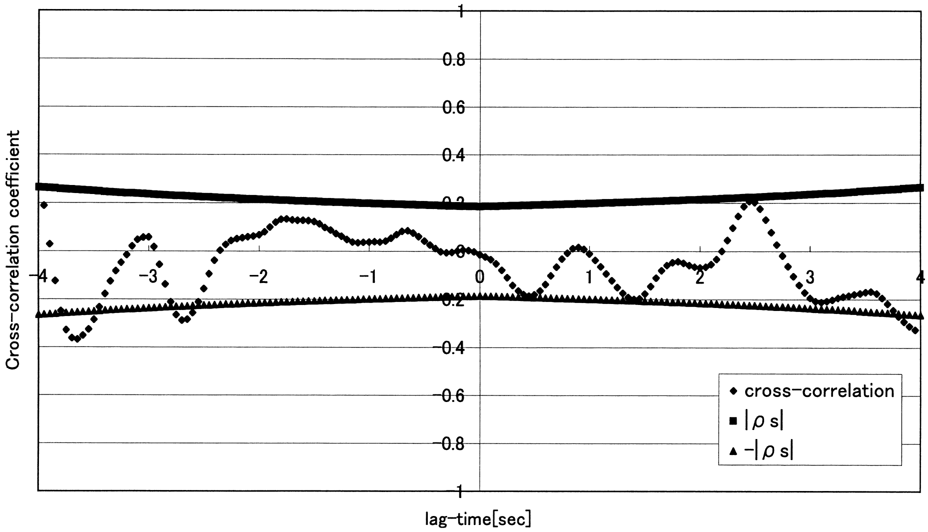

Fig. 9. We analyzed the time series data $\{(x_t, y_t)\}_{t\in K}$ for each 8 [s] with Measurement 2. Subject was S.I. (22 years old) with his eyes closed. We show a typical cross-correlation function between $\{x_t\}_{t\in K}$ and $\{y_t\}_{t\in K}$, and the significance levels of each correlation coefficient. We couldn't find significant correlation coefficients.

(positional receptors) in sole part is output to motor nerves (motorial position receptors) through central nerves (Cerebellum) (WILLIAM, 1999). We call this time interval nerve-response-time (NRT). We have considered that calculating the correlation for a long time is not necessary for analyzing the nerve response concerning the control of an upright position. We calculated the cross-correlation functions of the time series for 8 [s] in the data obtained with Measurement 2 for each subject and Q. The time length for 8 [s] is 100 times than the NRT mentioned above and it is very long time to analyze the nerve response. Each significance level of the correlation coefficient $|\rho_s|$ that depended on degree of freedom $N - k$ could be used since distributions of each time series $\{x_t\}_{t\in K}$, $\{y_t\}_{t\in K}$, where K was this time extent, fit normal distributions by tests of goodness of fit (Appendix C). Inequality $|\rho_{xy}(k)| \le |\rho_s|$ was satisfied for 50 [ms] $\le k \le$ 8 [ms] (Fig. 9), where 50 [ms] meant the sampling time on Measurement 2 and the time length for 8 [s] was the time extent on the calculation of $\rho_{xy}(k)$. Therefore, we could consider the processes $X(t)$ and $Y(t)$ as independent. We assume that individual mathematical models corresponding to each coordinate can describe them separately.

Next, we verify suitability for the assumptions in Section 4 with time series data $\{x_t\}_{t\in K}$ and $\{y_t\}_{t\in K}$ obtained with Measurement 2 for each subject and Q. It has been calculated that the stationary autocorrelation function on Markovian decays exponentially (GARDINER, 1983). Assumption 1 and 2 are examined with each verification:

Verification of Assumption 1 The autocorrelation function of time series $\rho_{xx}(k)$ decreases exponentially and falls below $1/e$ after that, where k means lag-time.

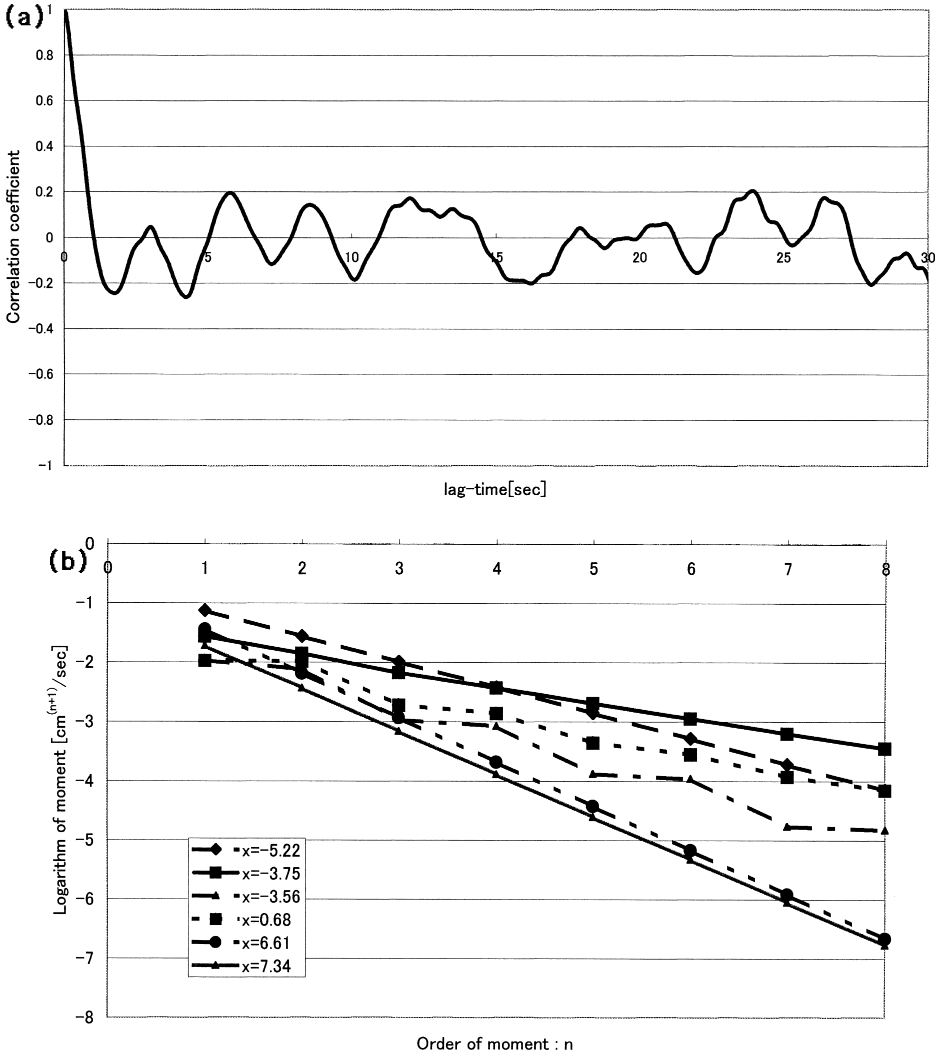

Fig. 10. We have verified whether the assumptions are suitable to the process that describes the time series data $\{(x_t, y_t)\}_{t\in K}$ of the sway. We analyzed the time series data with Measurement 2. Subject was T.N. (25 years old): (a) With his eyes closed. We show a typical graph of the autocorrelation function on $\{x_t\}_{t\in K}$. This autocorrelation function decreased exponentially and fell below $1/e$ after that. (b) With his eyes open. We show typical numerical integrations of $M_n(x)$ on $\{x_t\}_{t\in K}$.

Verification of Assumption 2 Numerical integrations of the moments of transition probability:

$$M_n(x) = \sum_{z\in\Omega} (z-x)^n P_{z,x}(t) W / \tau$$

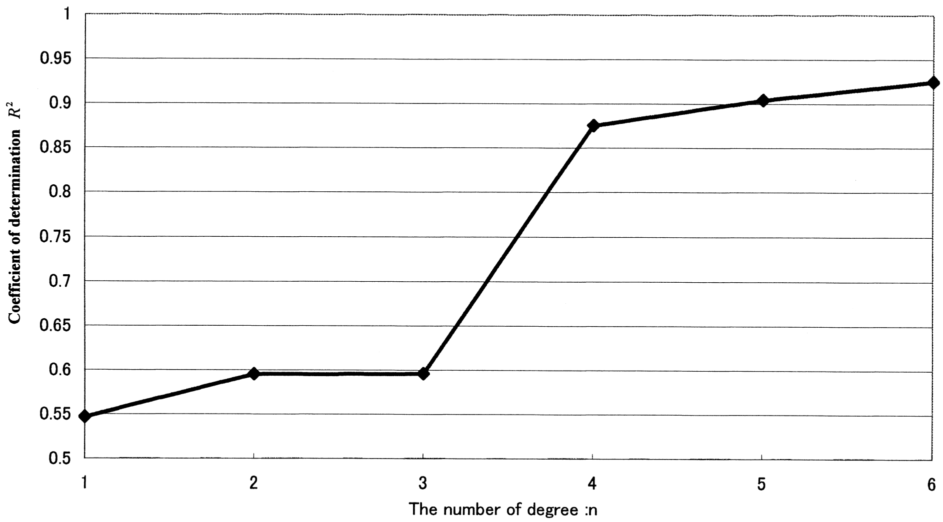

Fig. 11. We show a typical relation between the number of degree on the regression polynomial and the coefficient of determination on its regression of the LNH on the time series $\{\tilde{y}_t\}_{t\in K}$ (see Fig. 12).

$$\text{s.t.}\quad P_{z,x}(\tau) = \left.\frac{\#\{(X_t = x)\cap(X_{t+\tau} = z)\}}{\#(X_t = x)}\right|_{t\in K},$$

converge zero as n increases, where character # means "the number of", W is the minimal reading scale of the system (0.01 [cm]) and τ is the sampling time (50 [ms]).

The results of Verification of Assumptions 1 and 2 are shown in Fig. 10. Then, we could consider that Assumptions 1 and 2 were suitable to the process that describes the time series data of the sway of the center-of-gravity. In the following, we treat the process of the sway as a Markov process.

5.2. *Construction of the approximate mathematical model*

We assumed that the process of the sway was in a certain dynamical equilibrium state. Based on the theory in Section 4, the mathematical model can be constructed, because of the independency of the coordinates x, y. Before we lead a mathematical model that describes the process of the sway with our theory.

- We have standardized each time series $\{x_t\}_{t\in K}$, $\{y_t\}_{t\in K}$. These standardized time series are assumed to be $\{\tilde{x}_t\}_{t\in K}$, $\{\tilde{y}_t\}_{t\in K}$.
- We have regressed logarithmic normalized histograms on each standardized time series with graphs of each polynomial of degree n. We calculated each coefficient of determination R (KENDALL, 1958).

The following stochastic dynamical equation system (SDES) could be led approximately

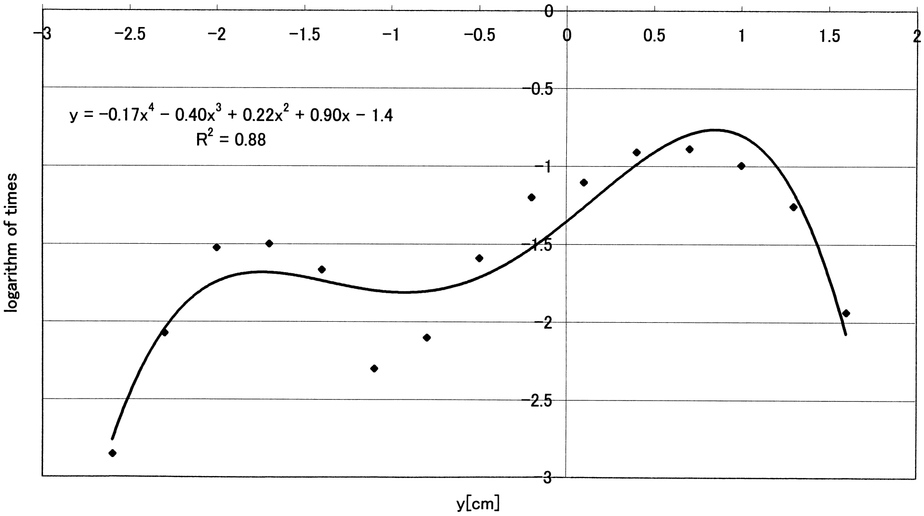

Fig. 12. We analyzed the time series data with Measurement 2. The subject was S.I. (22 years old) with eyes opened. We show the regression of the LNH on the time series $\{\tilde{y}_t\}_{t\in K}$ with the graph of a polynomial of degree 4.

as a mathematical model that described the process of the sway with the regression polynomial:

$$\frac{d}{dt}\begin{bmatrix} x \\ y \end{bmatrix} = \frac{1}{2}\sum_{k=1}^{n}\begin{bmatrix} ka_k^1 x^{k-1} \\ ka_k^2 y^{k-1} \end{bmatrix} + \begin{bmatrix} F^1(t) \\ F^2(t) \end{bmatrix},$$

where $F^1(t)$ and $F^2(t)$ are independent and the standardized fluctuating force generated with the Gauss type stochastic process. $a_k{}^1$ and $a_k{}^2$ are regression coefficients of the polynomial for k (a natural number) on the regression with the least square method. The value R is useful when one is considering the suitability for the regression curve and the relative importance on correlations of different magnitudes (ROBERT and JAMES, 1969). The relation between n and R on each regression of the logarithmic normalized histogram (LNH) is shown in Fig. 11. R tended to 0.9 at $n = 4$ and was sufficiently large there. With the relation obtained by differentiating both sides of Eq. (7), we could consider that each time-averaged equilibrium space on the SDES was approximated sufficiently with the graph of a polynomial of degree 3.

The LNH on the time series $\{\tilde{y}_t\}_{t\in K}$ of a certain subject with eyes opened (obtained with Measurement 2) and its typical regression with the graph of a polynomial of degree 4 is shown in Fig. 12. We could admit the similar form of the LNH on the time series $\{\tilde{x}_t\}_{t\in K}$ and the graph of the polynomial of degree 4 as its regression curve. Here, coefficients of the regression polynomial were as follows:

$$\frac{d}{dt}\begin{bmatrix} x \\ y \end{bmatrix} = \frac{1}{2}\sum_{k=1}^{4}\begin{bmatrix} ka_k^1 x^{k-1} \\ ka_k^2 y^{k-1} \end{bmatrix} + \begin{bmatrix} F^1(t) \\ F^2(t) \end{bmatrix}, \tag{9}$$

where

$$\begin{pmatrix} a_1^1 & a_2^1 & a_3^1 & a_4^1 \\ a_1^2 & a_2^2 & a_3^2 & a_4^2 \end{pmatrix} = \begin{pmatrix} 0.10 & -0.30 & -0.0019 & 0.0075 \\ 0.90 & 0.22 & -0.40 & -0.17 \end{pmatrix}.$$

5.3. Numerical simulations of our mathematical model

We employed numerical simulations of the SDES obtained with data recorded with Measurement 2 on each subject and Q. We rewrote Eq. (9) into the difference equation and obtained numerical solutions with the Runge-Kutta-Gill formula as the numerical calculus.

(a)

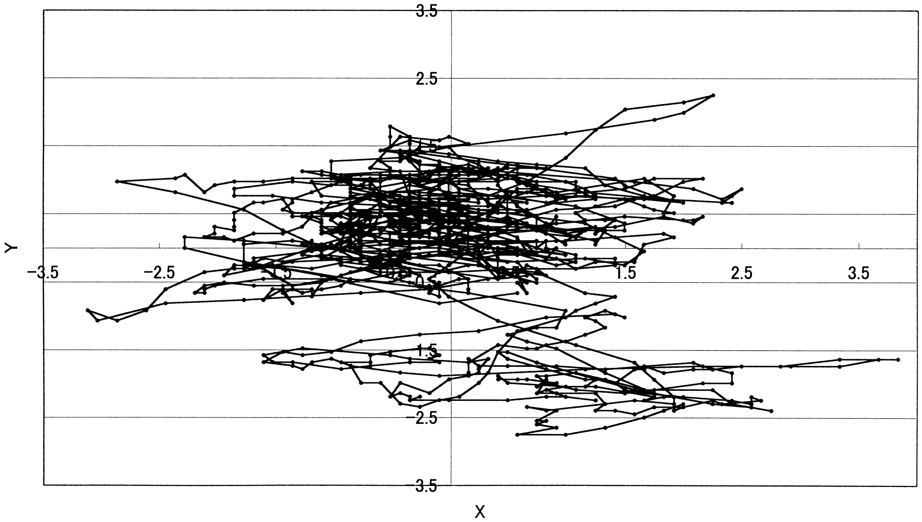

Fig. 13. We show typical statokinesigrams obtained with the time series data $\{(\tilde{x}_t, \tilde{y}_t)\}_{t\in K}$ (a) and the numerical computation (b). (a) The subject was S.I. (22 years old) with his eyes open. (b) We calculated the numerical simulation on Eq. (9) describing the time series data $\{(\tilde{x}_t, \tilde{y}_t)\}_{t\in K}$. The initial condition (1.91–2.39) was given by $\{(\tilde{x}_t, \tilde{y}_t)\}_{t\in K}$. We used pseudo random number series obtained by the linear congruential method (LEHMER, 1951). Two series of the pseudo random numbers whose domain was [0,1) were standardized respectively for this numerical computation. Based on the observation theory, we estimated each standard deviation on the displacement for a time step (0.05 [s]) with $\{\tilde{x}_t\}_{t\in K}$, $\{\tilde{y}_t\}_{t\in K}$ and normalized series of the pseudo random numbers with each standard deviation (TAKADA, 2001). We introduced these series into the white noise terms on the difference equation system that we rewrote Eq. (9) into. We calculated this system with the Runnge-Kutta-Gill formula by the time step 0.05.

Here, we mention a typical numerical solution on the SDES Eq. (9) although we have admitted same results of the calculation for the others.

We can compare the pattern on *X-Y* recording (statokinesigram) of the data of the sway with the statokinesigram of the numerical simulation in Fig. 13. The same type of *polarity* and *rhythm* on the *force* acting on the center-of-gravity were reproduced well with the simulation (Fig. 14).

However, the following features seemed to be difficult to express with the simulation.

1) Smooth rotation movement.
2) Suddenly stopping after straight sway and turning.
3) Appearance of extremely large and small velocity vectors.

For especially 1), we calculated distributions of the rotation angles on the data of the sway and the numerical simulation (Fig. 15). It was likely that the distribution of the rotation angles on the simulation was almost uniform since we assumed independent coordinates in our mathematical model. Then, we have employed the tests of goodness of fit for this verification:

(A) Whether the distribution of simulated rotation angles fits a uniform distribution.
(B) Whether the distribution of observed rotation angles fits a uniform distribution.

It is the null hypothesis on (A) that the distribution of simulated rotation angles fits a uniform distribution and on (B) that on the observed data also fits it. As a result, the former was accepted and the latter was not with a significance level 0.05 (Appendix C).

Though the distribution of simulated rotation angles was assumed to be the uniform distribution, that observed with Measurement 2 was not assume to be it; therefore it could not be said that distributions of the rotation angles on the observed data and the numerical simulation were same.

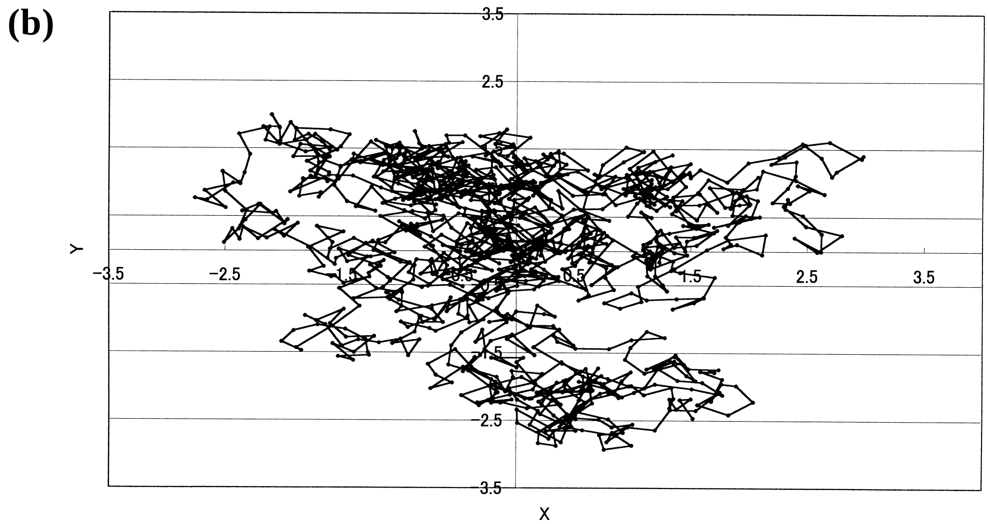

Fig. 13. (continued).

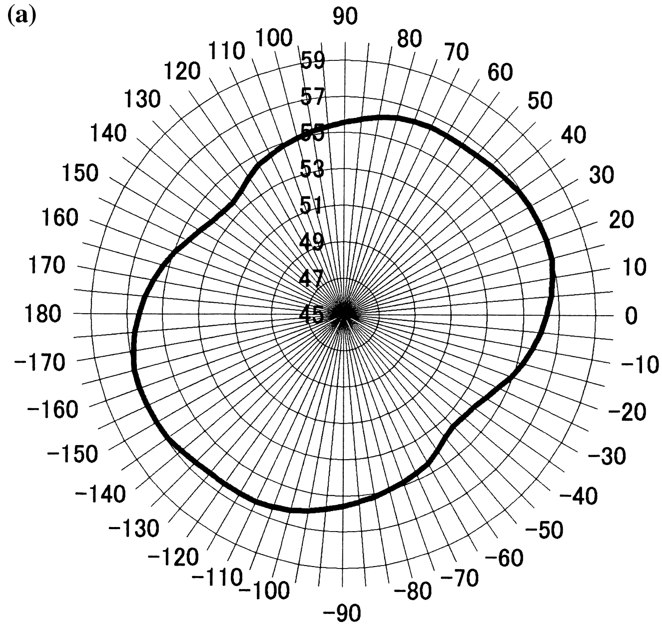

Fig. 14. We examined whether the numerical solution that was shown in Fig. 13(b) had the polarity and the *rhythm* on the *force* acting on the simulated center-of-gravity. (a) We show each sum total of force onto the direction of angle *j*° on this series. (b) We show moving averages on the sum total of force onto the direction of 0° on this series.

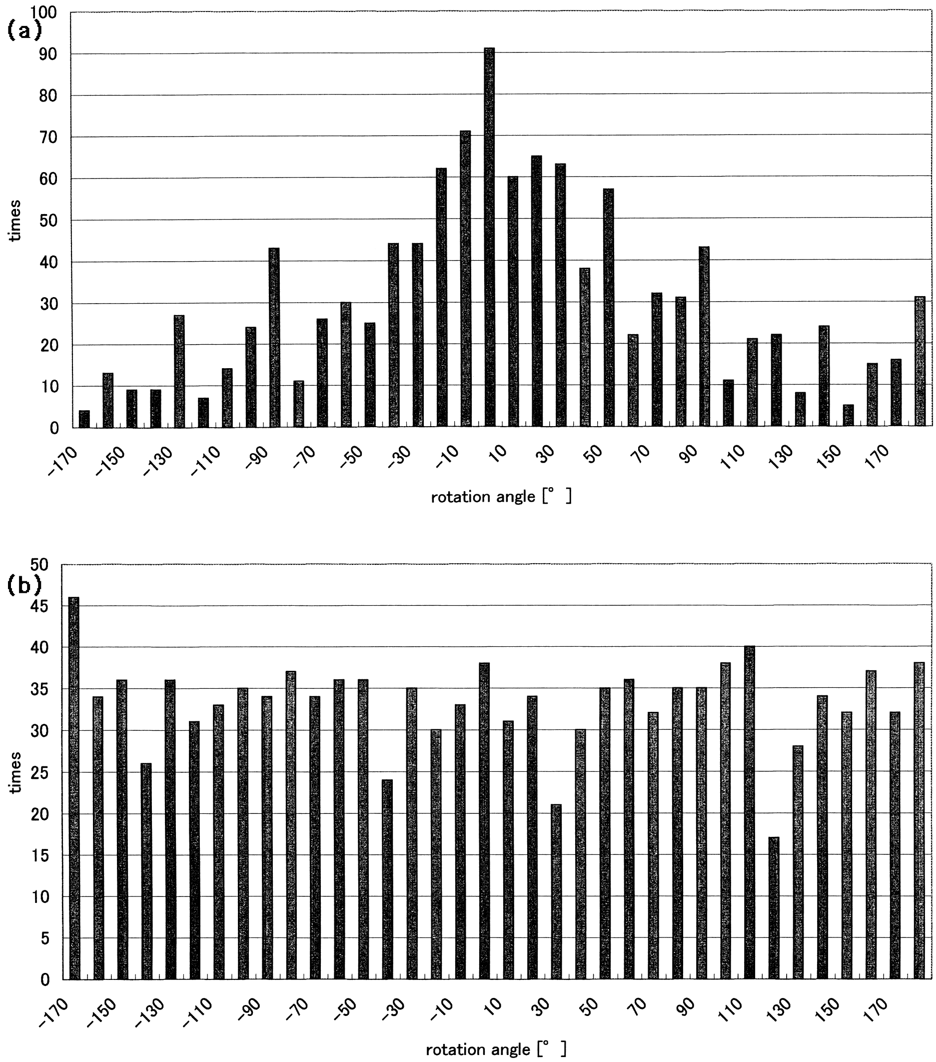

Fig. 15. We show typical distributions of the rotation angles on the observed data of the sway (a) and the numerical simulation (b). (a) The subject was S.I. (22 years old) with his eyes open. (b) The numerical solution used in this analysis was shown in Fig. 13(b).

6. Consideration

6.1. Polarity and rhythm of force

By the analysis in Section 3, the *force* acting on the center-of-gravity of each subject who had visual information was smaller than who didn't have it at the first experiment (M = 1, 2). We could consider the following contexts:

- The *force* was not a constant but increased relatively by repetition of experiments. At the third experiment ($M = 5, 6$), force applied on the subject who had visual information exceeded the force exerted on the subject who had no visual information (Subsection 3.1, Fig. 5).
- In any directions, the variations per unit time for the time extent when the subject stood with visual information were slower than when he stood without (Subsection 3.2, Fig. 7).

We could admit a certain kind of *polarity* and *rhythm* on the *force* though there were individual variations. When the subject stood with visual information,

- Rotation on the *direction of polarity* was admitted (Fig. 4(b)).
- The periods on the *sum total of force* were longer than without it (Fig. 7).

The possibility is suggested that the control on man's standing posture with visual information constructs smooth and slow minute disturbance on the center-of-gravity. This verification is a problem in future.

The same type of *polarity* and *rhythm* on the *force* acting on the center-of-gravity were reproduced well with our simulation. Our theory contains not only the OU process but also other processes and the potential function in the meaning of the time average on our model accepted in Subsection 5.2 is the polynomial of degree 4. This time-averaged potential has not only a minimal point but also some minimal points. We have supposed that this structure generates the *polarity* in spite of independence of each coordinate x, y and the standardized fluctuating force $F^1(t)$, $F^2(t)$.

6.2. Comparison of the previous model with our mathematical model

Many stochastic models have been proposed such as the random-walk model by COLLINS and DE LUCA (1993), EMMERIK *et al*. (1993) and NEWELL *et al*. (1997). These models are based on the OU process. The process is generated by the SDE (6) and has been solved strictly by the Fokker-Plank equation (Appendix B). The OU process is well known as a mathematical model that describes irregular movement of a minute particle floating in liquid, what is called Brownian motion. According to Einstein relation (EINSTEIN, 1905), mean square displacement $\langle \Delta x^2 \rangle$ of a one-dimensional random walk is proportional to the time interval Δt:

$$\left\langle \Delta x^2 \right\rangle = 2D\Delta t, \tag{10}$$

where the parameter D is the diffusion coefficient. Fractional Brownian motion was introduced by MANDELBROT and VAN NESS (1968). Equation (10) for this motion has been generalized to the following scaling law:

$$\left\langle \Delta x^2 \right\rangle \approx \Delta t^{2H}, \tag{11}$$

where the scaling exponent H can be any real numbers in the range: $0 < H < 1$. For the ordinal Brownian motion, $H = 1/2$.

Especially, COLLINS and DE LUCA (1993) found Eqs. (10) and (11) on the sway of the center-of-gravity with their time series data. The following contents were clarified by this work:

- They found two term regions on the time interval: a short-term region and a long-term region. Equation (10) was satisfied for each term region. It is possible to describe the sway of the center-of-gravity by the stochastic process that describes the Brownian motion with the restriction on the local time interval to analyze.
- They found the values D, H for each term region by using Eqs. (10) and (11). On the global term region, their results were qualitatively different from those expected for the ordinary Brownian motion.

We have tried to consider theoretical extension on the stochastic model that describes the sway of the center-of-gravity though our model is also based on the stochastic process theory. Our theory contains not only the OU process but also further processes that are included in a countable-infinite set. We consider the control system on the sway of the center-of-gravity in a certain dynamical equilibrium state. Based on the time series data, we have led that the potential function in the meaning of the time average is not a parabolic function that describes the OU process, but it must be expressed by a polynomial whose order is larger than 4. Moreover, the potential function must be forth order if it is structural stable. We do not mention the necessity of the number of its order with the consideration on the structural stability (TAKADA, 2001), but the sufficiency for simplification here.

As mentioned in Subsection 5.1, the distributions of each time series $\{x_t\}_{t\in K}$, $\{y_t\}_{t\in K}$ where K was the local time extent fit normal distributions by the tests of goodness of fit. The fact is not against the previous work mentioned above. But according to stabirometry, one cannot look into the control system on the sway of the center-of-gravity in a certain dynamical equilibrium state with the time series data for the local time extent empirically. It takes 60 [s] to analyze the control system (SUZUKI *et al.*, 1996). Based on their insistence, our mathematical model was obtained by referring to the time series data for 60 [s], long time extent to analyze the control system. We regressed the logarithmic normalized histograms on each standardized time series $\{\tilde{x}_t\}_{t\in K}$, $\{\tilde{y}_t\}_{t\in K}$ with the graphs of polynomials. Coefficients of determination R on each regression were shown in Fig. 11. R on the regression with the graph of a polynomial of degree 4 was about 0.9 though with the parabolic curve was less than 0.6. The regression curve must be the graph of the polynomial whose order is larger than 4 if R as determination force is assumed to be more than 0.9. Then, Eq. (6) obtained by the regression with the parabolic curve is not appropriate as a mathematical model of the sway of the center-of-gravity.

We compared the results of the numerical calculation on Eq. (6) derived by the method in Subsection 5.2 with Eq. (9) and evaluated which of these differential equations was appropriate as a mathematical model on the sway of the center-of-gravity. We regressed the LNH on each standardized time series with the parabolic curve.

$$\frac{d}{dt}\begin{bmatrix} x \\ y \end{bmatrix} = \begin{bmatrix} 0.058 - 0.21x \\ 0.064 - 0.13y \end{bmatrix} + \begin{bmatrix} F^1(t) \\ F^2(t) \end{bmatrix} \tag{12}$$

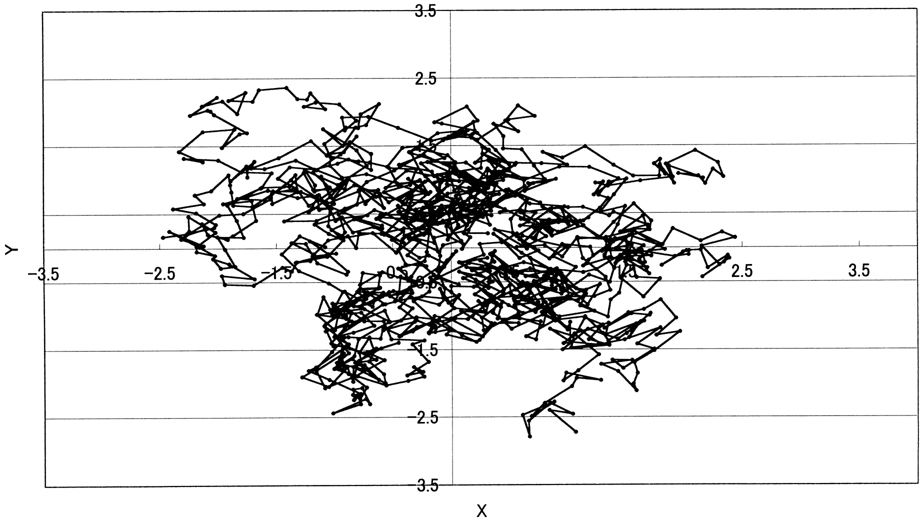

Fig. 16. We show a typical statokinesigram obtained with the numerical simulation on Eq. (12) for the comparison of the previous model with our model. The method of the numerical simulation and its initial condition were same as the calculation on Fig. 13(b).

as same as the previous work, was derived by our theory. We calculated numerical simulations on Eq. (12) with the formula in Subsection 5.3 (Fig. 16). Any cross-correlation coefficients between each time series data $\{\tilde{x}_t\}_{t\in K}$, $\{\tilde{y}_t\}_{t\in K}$ and the time series generated by these computations were less than 0.23 though the coefficients between each time series data and the time series generated by the numerical simulations in Subsection 5.3 reached 0.71. Therefore, the mathematical model of the sway of the center-of-gravity has been improved by our theory.

6.3. Our mathematical model and its simulation

On Assumptions 1 and 2, we have obtained the mathematical model that describes the process of the sway as an element of the set of Fokker-Plank equations. The FPE is solvable under certain conditions (Appendix B). We have shown that an element of the set of stochastic dynamical equations corresponding to the FPE that describes the process is led uniquely in our theory.

We have constructed stochastic dynamical equations on some time series data besides the sway of the center-of-gravity of the body as a mathematical model with this theory. Here, we compared them to evaluate the degree of the explanation on this mathematical model and understand the complexity of phenomenon. For example, we have obtained a SDE corresponding to exchange rates (¥/$) and its numerical simulation (TAKADA *et al.*, 1999). The cross-correlation coefficient between the time series of exchange rates and its numerical solution was about 0.88. The cross-correlation coefficient between the time series of the sway of the center-of-gravity of the body and our numerical solution was less than 0.71 mentioned above. Therefore, we could admit that the time series on the sway of the center-of-gravity in the living body mechanism was not well described as the time series of exchange rates in economy with this theory. We considered that one of the reasons why the process of the sway was not reproduced sufficiently in this research might be our overlooking of the significant cross-correlation coefficient $\rho_{xy}(k)$ for $k < 50$ [ms] and $k >$ 8 [s]. 50 [ms] is the sampling time on Measurement 2. We calculated the cross-correlation functions of the time series for 8 [s] to analyze the nerve response.

In general, we can consider that unexpected fluctuating behavior that depends on components is described by the white noise. A SDE that describes the process is an approximation on the dynamical system in high dimensional space. When we lead the SDE corresponding to a FPE, a problem of rule-of-calculation appears if the coefficient of the white noise term depends on the random variable though the rule-of-calculation has not directly participated in this theory. The permutation of variables Eq. (B1) is effective only if we limit on Stratonovich's rule that treats only Newtonian differentiation. Then, this rule was required for theoretical correspondence in this theory.

However, we considered that failure of this rule was suggested as another reason why the process of the sway was not reproduced sufficiently in this research. In some phenomena besides this, using other rule like Ito calculus is often effective (ITO, 1944; DOOB, 1953). We should judge what is adopted with comparison of the real data with stochastic processes led with either of the two rules (MORTENSEN, 1969). A construction of the theory with Ito calculus and comparison of this numerical solution besides that in Subsection 5.3 with the observed data of the sway of the center-of-gravity in human's standing posture are problem in future.

Moreover, a type of the SDE that depends on the random variable and fluctuation force at the past time as follows may describe the stochastic process:

$$\frac{dz}{dt} = G\left(\hat{a}(z), F_0(t), \ \ldots, \ F_k(t)\right),$$

where k is less than N that is the number of data points, and $F_k(t)$ is fluctuation force before k units of time step. Problems in future are a construction of the theory that lead the SDE mentioned above and a verification of the suitability for the obtained mathematical model.

7. Conclusion

We analyzed the sway of the center-of-gravity of the body by paying attention to *force* acting on it. We clarified the following characters:

1. *Polarity* and *rhythm* exist on the force.
2. Rotation on the *direction of polarity* with visual information.
3. Periods of the *sum total of force* with visual information is longer than without it.

We have obtained a stochastic dynamical equation system (SDES) as a mathematical model that describes the process of the sway from obtained data on Assumptions 1 and 2. We compared the numerical solution of SDES based on the obtained data with it and examined suitability for the model. Some characters, like the *rotation angle*, were not sufficiently reproduced with the model. A construction of the mathematical model that describes such detail characters is a problem in future.

We would like to thank Prof. S. Mori of Nagoya University and Dr. S. Ichikawa for their offer of the medical equipment (Force Plate) on sampling the sway of the center-of-gravity of the body. We also express our thanks to Prof. Y. Shikata of Meijo University for guidance of this interesting problem and Prof. K. Mihashi of Nagoya University for his useful discussion and advice on English.

Appendix A: Basic Equations on Markovian

The Markov process is a case that the probability distribution of a continuous process $X(t)$ depends on t and $X(t_0)$ in $t > t_0$, and it does not depend on $X(t)$ in $t < t_0$. The Chapman-Kolmogorov equation is a mathematical expression of Assumption 1:

$$P(x|y, t_1 + t_2) = \int_\Omega P(x|z, t_2) P(z|y, t_1) dz. \tag{A1}$$

Here, we apply the following theoretical conditions to Eq. (A1).

1. The probability distribution does not change remarkably in short time.
2. The initial condition such that the random variable is y in the beginning:

$$\lim_{t \to 0} P(x|y, t) = \delta(x - y),$$

where $\delta(x)$ is Dirac's delta function for any real numbers x. The following Kramers-Moyal expansion is derived by expanding Eq. (A1) into Taylor series under above conditions (RISKEN, 1984):

$$\frac{\partial P(x|y, t)}{\partial t} = \sum_{n=1}^{\infty} \frac{(-1)^n}{n!} \frac{\partial^n}{\partial x^n} \left[M_n(x) P(x|y, t) \right] \tag{A2}$$

$$\text{s.t.} \quad M_n(x) = \lim_{\tau \to 0} \frac{1}{\tau} \int_\Omega (z - x)^n P(z|x, \tau) dz, \tag{A3}$$

where n is any natural numbers. Equation (A2) is a stochastic differential equation that describes the process. The following theorem concerning the moment of transition probability $M_n(x)$ on Markovian is given in the stochastic process theory.

Theorem A.1 (PAWULA, 1967) The moment of transition probability $M_n(x)$ for degree n (a natural number) satisfies at least either condition:

$$M_n(x) = \begin{cases} = 0 & (\text{where } n \text{ is any natural number more than 3}) \\ \neq 0 & (\text{where } n \text{ is any even number}), \end{cases}$$

as far as $M_n(x)$ exists for all n.

If $M_n(x)$ is not 0 but a finite value for large n, $X(t)$ must be an anomalous process that extends far rapidly in short time. We suppose Assumption 2 in this theory for a demand on physics. Therefore $M_n(x)$ is zero ($n > 2$) on Assumption 2. Equation (A2) can be rewritten into the following Fokker-Plank equation.

$$\frac{\partial P(x|y,t)}{\partial t} = -\frac{\partial}{\partial x}\left[a(x)P(x|y,t)\right] + \frac{1}{2}\frac{\partial^2}{\partial x^2}\left[b(x)P(x|y,t)\right]. \tag{A4}$$

The moment (A3) becomes the following with the calculation based on Eq. (A4) (TAKADA, 2001).

Proposition A.2 $M_1(x) = a(x)$, $M_2(x) = b(x)$ and $M_n(x) = 0$ ($n \geq 3$).

With the last formula, we can consider that the stochastic process $X(t)$ on Eq. (A4) is not an anomalous-diffusion process. We treat such processes in this paper.

Appendix B: Application of Fokker-Plank Equations and Their Solutions

Since Fokker-Plank equations are solvable under certain conditions, returning to a FPE is effective to discuss the model. Solution of the FPE is obtained with the permutation of variables:

$$dz = \frac{dx}{\beta}, \quad \hat{a}(z) = \frac{\alpha(x(z))}{\beta(x(z))} \quad \text{s.t.} \quad \alpha(x) \equiv a(x) - \frac{1}{4}\frac{\partial b(x)}{\partial x}, \quad \beta(x)^2 \equiv b(x). \tag{B1}$$

Equation (A4) goes over into:

$$\frac{\partial g(z|z_0,t)}{\partial t} = -\frac{\partial}{\partial z}\left\{\hat{a}(z)g(z|z_0,t)\right\} + \frac{1}{2}\frac{\partial^2}{\partial z^2}g(z|z_0,t) \equiv -\frac{\partial}{\partial z}J(z|x,t), \tag{B2}$$

where the stationary flow of the probability $J(z|x, \infty) = J(\infty)$ is a constant (GOEL and RICHTER-DYN, 1978). The solution of Eq. (B2) is obtained by the separation of variable in the quantum theory. Substituting the test function $g(z|z_0, t) = \psi(z)\sqrt{C\exp[-Et]/g(z)}$ in Eq. (B2), this equation goes over into a time-independent Schrödinger equation (SE):

$$\frac{d^2\psi(z)}{dz^2} + \left[E - U(z)\right]\psi(z) = 0$$

$$\text{s.t.} \quad U(z) = \frac{\partial}{\partial z}\hat{a}(z) + \hat{a}(z)^2.$$

The following theorem is effective to obtain the solution of the SE:

Theorem B.1 (TITCHMARSH, 1962) $\{E_n, \psi_n(z)\}$, the set of eigenvalues and eigenfunctions beside the eigenvalue problem of the SE, are discrete and $\{\psi_n(z)\}$, the set of functions, is the orthonormal system if the variable z is limited with two boundaries and the potential function $U(z)$ is a bounded function in these boundaries.

Solutions of Fokker-Plank equations on some types of the function $\hat{a}(z)$ could be obtained (STRATTON *et al*., 1956; MAGNUS *et al*., 1966). For instance, the solutions of any Fokker-Plank equations that describe the OU processes have been solved by using the Hermite polynomial under some boundary conditions (ABRAMOWITZ and STEGUN, 1964).

A strict stationary solution of Eq. (B2) can be obtained. The SPDF that describes the process in a certain dynamical equilibrium state is assumed to be $g(z) \equiv g(z|z_0, \infty)$ in Eq. (B2). Since partial differentiation of time of $g(\partial g/\partial t)$ is equal to 0, the stationary solution of Eq. (B2) is obtained by solving the following first-order linear differential equation:

$$-2\hat{a}(z)g(z) + \frac{dg(z)}{dz} = -2J(\infty).$$

Solving this differential equation with the separation of variables, Theorem 1 is obtained.

Appendix C: Tests of Goodness of Fit

If following Eq. (C1) is hold, the hypothesis $p_i = p_i^0$ is supported with a significance level α:

$$\sum_{i=1}^{k} \frac{\left(x_i - np_i^0\right)^2}{np_i^0} < \chi_{k-1}^2(\alpha), \tag{C1}$$

where k is the number of classes on a histogram, x_i is the frequency of the class i, p_i is the PDF obtained from the data such as positions, rotation angles, $\chi_{k-1}{}^2(\alpha)$ is the chi-square distribution (ROBERT and JAMES, 1969) and p_i^0 is the following probability distribution.

- The normal distribution whose average and dispersion are equal to those of the testing population in Subsection 5.1.
- The uniform distribution in Subsection 5.3.

A significance level of the correlation coefficient is led with the acceptance of the former. Z-transformation of r is assumed to be the normal distribution whose mean value is $\tanh^{-1}\rho$ and standard deviation is $1/\sqrt{N-3}$, where r is a sample correlation function of N-pair samples extracted arbitrary from the bivariate normal population with the population correlation coefficient ρ (ROBERT and JAMES, 1969). If a significance level on this normal distribution is given, the significance level of the correlation coefficient can be calculated. Here, we take this statistical test on the latter as follows.

1) We have employed a test of goodness of fit whether the distribution of the simulated rotation angles fits a uniform distribution. The value of the left side of Eq. (C1) was 29.29 at intervals of 10° (with degree of freedom as 35). The value of the right side of Eq. (C1) was 49.80 for $\alpha = 0.05$ and Eq. (C1) held on. Hence, the null hypothesis that the distribution of the simulated rotation angles fits a uniform distribution has been accepted.

2) We have employed a test of goodness of fit whether the distribution of the observed rotation angles fits a uniform distribution. The value of the left side of Eq. (C1) was 526.48 with the same class step as 1). Equation (C1) did not hold on with the significance level 0.05; therefore the null hypothesis that the distribution of the observed rotation angles fits a uniform distribution has been rejected.

REFERENCES

ABRAMOWITZ, M. and STEGUN, I. A. (eds.) (1964) *Handbook of Mathematical Functions*, Nat. Bur. Stand., Washington, D.C.

COLLINS, J. J. and DE LUCA, C. J. (1993) *Experimental Brain Research*, **95**, 308–318.

DOOB, J. L. (1953) *Stochastic Process*, John Wiley & Sons, Inc., New York, p. 273.

EINSTEIN, A. (1905) *Ann. Phys*., **322**, 549–560.

EMMERIK, R. E. A., VAN SPRAGUE, R. L. and NEWELL, K. M. (1993) *Moving Disorders*, **8**, 305–314.

GARDINER, C. W. (1983) *Handbook of Stochastic Methods*, Springer-Verlag.

GOEL, N. S. and RICHTER-DYN, N. (1978) *Theory of Stochastic Process in Biology*, Industrial Books.

HARKEN, H. (1975) *Rev. Mod. Phys*., **47**, 67.

ITO, K. (1944) Stochastic integral. *Proc. Imp Acad. (Tokyo)*, **20**, 519.

KENDALL, M. G. and STUART, A. (1958–63) *The Advanced Theory of Statistics, I–III*, Charles Griffin & Company Ltd., pp. 412–413.

LEHMER, D. H. (1951) *Ann. Comput. Lab. (Harvard University)*, **26**, 141–146.

MAGNUS, W., OBERHETTINGER, F. and SONI, R. P. (1966) *Formulas and Theorems for the Special Functions of Mathematical Physics*, Springer-Verlag, Berlin and New York, pp. 7–9, 50, 76, 79, 83.

MANDERBLOT, B. B. and VAN NESS, J. W. (1968) *SIAM Rev*., **10**, 422–437.

MORI, M., TOKITA, T., OKAWA, T., SHIBATA, Y. and MIYATA, H. (1998) *Equilibrium Res*., **57**(6), 556–565.

MORTENSEN, R. E. (1969) Mathematical problem of modeling stochastic nonlinear dynamic systems. *J. Statist. Phys*., **1**, 271.

NEWELL, K. M., SLOBOUNOV, S. M. and SLOBOUNOVA, E. S. (1997) *Stochastic Processes in Postural Center-of-Pressure Profiles*, Vol. 133.

PAWULA, R. F. (1967) *Phys. Rev*., **162**, 196.

POSTON, T. and STEWART, I. (1978) *Catastrophe Theory and Its Applications*, Pitman Publishing Ltd.

RISKEN, H. (1984) *The Fokker-Plank Equation-Methods of Solution and Applications*, Springer-Verlag, pp. 67–69.

ROBERT, R. S. and JAMES, R. F. (1969) *Introduction to Biostatistics*, W.H. Freeman and Company.

SHIKATA, A., TAKADA, H., MORI, S. and SHIKATA, Y. (1997) *Ann. Res. Inst. Environ. Med. Nagoya Univ*., **47**, 27–29.

STRATONOVICH, R. (1963) *Topics in the Theory of Random Noise, 1*, Gordon & Breach, New York, p. 59.

STRATTON, J. A., MORSE, P. M., CHU, L. J., LITTLE, J. D. C. and CORBATO, F. J. (1956) *Spheroidal Wave Functions*, Thchnol. Press of MIT, New York, p. 2.

SUZUKI, J., MATSUNAGA, W., TOKUMASU, A., TAGUCHI, K. and WATANABE, I. (1996) *Equilibrium Res.*, **55**(1), 64–77.

TAKADA, H. (2001) Construction method of the mathematical model on time series data with Markov property and verification, Ph.D. Thesis, Nagoya University (in preparation).

TAKADA, H. and SHIKATA, Y. (1998) *Research on the Establishment and Education of Mathematical Science*, 288–298 (in Japanese).

TAKADA, H., SHIMIZU, Y., YOSHIMORI, M. and MATSUGI, T. (1999) *Bulletin of Society for Science on Form*, **14**(3), 208–209 (in Japanese) .

TAKEUCHI, J., YAMAMOTO, M. and YOSHIDA, T. (1997) *Equilibrium Res.*, **56**(3), 129.

TITCHMARSH, E. C. (1962) *Eigenfunction Expansions Associated with Second-Order Differential Equations*, Oxford Univ. Press (Clarendon), London and New York, pp. 107–110.

WILLIAM, F. G. (1999) *Review of Medical Physiology* 19th Ed., 57, Prentice-Hall international.